Electrophysiological network alterations in adults with copy number variants associated with high neurodevelopmental risk

Diana C. Dima[1,2*], Rachael Adams[1,3], Stefanie C. Linden[2,3,4], Alister Baird[3], Jacqueline Smith[3,4], Sonya Foley[1], Gavin Perry[1], Bethany C. Routley[1], Lorenzo Magazzini[1], Mark Drakesmith[1,2], Nigel Williams[2,3,4], Joanne Doherty[1,3,4], Marianne B.M. van den Bree[2,3,4], Michael J. Owen[2,3,4], Jeremy Hall[2,3,4], David E. J. Linden[1,2,3,4,5], and Krish D. Singh[1]

Author affiliations:

[1] Cardiff University Brain Research Imaging Centre (CUBRIC), School of Psychology, Cardiff University, Maindy Road, Cardiff, CF24 4HQ, United Kingdom

[2] Neuroscience and Mental Health Research Institute (NMHRI), Cardiff University, Maindy Road, Cardiff, CF24 4HQ, United Kingdom

[3] Division of Psychological Medicine and Clinical Neurosciences, School of Medicine, Cardiff University, Cardiff, CF24 4HQ, UK

[4] MRC Centre for Neuropsychiatric Genetics and Genomics, School of Medicine, Cardiff University, Maindy Road, Cardiff, CF24 4HQ, United Kingdom

[5] School of Mental Health and Neuroscience, Faculty of Health, Medicine and Life Sciences, Maastricht University, Maastricht, The Netherlands

*Corresponding author: DimaDC@cardiff.ac.uk

Abstract

Rare copy number variants associated with increased risk for neurodevelopmental and psychiatric disorders (referred to as ND-CNVs) are characterized by heterogeneous phenotypes thought to share a considerable degree of overlap. Altered neural integration has often been linked to psychopathology and is a candidate marker for potential convergent mechanisms through which ND-CNVs modify risk; however, the rarity of ND-CNVs means that few studies have assessed their neural correlates. Here, we used magnetoencephalography (MEG) to investigate resting-state oscillatory connectivity in a cohort of 42 adults with ND-CNVs, including deletions or duplications at 22q11.2, 15q11.2, 15q13.3, 16p11.2, 17q12, 1q21.1, 3q29, and 2p16.3, and 42 controls. We observed decreased connectivity between occipital, temporal and parietal areas in participants with ND-CNVs. This pattern was common across genotypes and not exclusively characteristic of 22q11.2 deletions, which were present in a third of our cohort. Furthermore, a data-driven graph theory framework enabled us to successfully distinguish participants with ND-CNVs from unaffected controls using differences in node centrality and network segregation. Together, our results point to alterations in electrophysiological connectivity as a putative common mechanism through which genetic factors confer increased risk for neurodevelopmental and psychiatric disorders.

Introduction

A number of rare genetic variants occurring through the deletion or duplication of chromosomal segments are associated with significantly increased risk for a range of neurodevelopmental disorders (ND), including schizophrenia, autism spectrum disorder (ASD), and developmental delay (Kirov et al., 2014). Although the underlying mechanisms remain poorly understood, these copy number variants (referred to hereafter as ND-CNVs) are thought to increase the risk for psychopathology through alterations in neural structure and function. Thus, neuroimaging studies in participants with ND-CNVs provide a unique opportunity to study intermediate phenotypes of mental disorders.

Recent work suggests that CNV-specific phenotypic outcomes are limited, pointing instead to a large degree of similarity across phenotypes associated with different ND-CNVs (Chawner et al., 2019; Niarchou et al., 2019). Focusing on convergent neural alterations across different genotypes can thus help elucidate the mechanisms linking ND-CNVs at different loci to a shared psychopathology and increase in neurodevelopmental risk.

Failures of functional neural integration are considered a hallmark of schizophrenia (Friston et al., 2016; Dong et al., 2018) and have also been found in ASD (Hull et al., 2017; O'Reilly et al., 2017) and across diagnostic boundaries (Sha et al., 2019). ND-CNVs are thought to increase disorder risk by acting on large-scale neural integration through molecular and cellular mechanisms (Karayiorgou et al., 2010). Synchronous oscillatory activity thought to support communication between brain areas is thus of particular interest as a potential biomarker of neurodevelopmental risk, and can be measured at rest using electro- and magneto-encephalography (EEG/MEG).

However, the rarity of ND-CNVs means that evidence of their functional connectivity correlates is scarce. Of the genetic imaging studies conducted so far, most have focused on the

22q11.2 deletion syndrome. This deletion is associated with a number of physical phenotype manifestations as well as high risk for psychopathology (Jonas et al., 2014; Niarchou et al., 2014; Schneider et al., 2014; Owen and Doherty, 2016). The presence of a 22q11.2 deletion has been linked to alterations in brain structure and function (Zinkstok and Amelsvoort, 2005; Boot and van Amelsvoort, 2013; Reddaway et al., 2018; Sun et al., 2018), including disrupted structural connectivity (Ottet et al., 2013; Villalón-Reina et al., 2019). Although fewer studies have investigated functional connectivity, they report similarly disrupted networks using functional MRI (Debbané et al., 2012; Padula et al., 2015; Scariati et al., 2016b) and EEG (Tomescu et al., 2014).

Despite emerging evidence of white matter alterations associated with other ND-CNVs (Berman et al., 2016; Drakesmith et al., 2019; Silva et al., 2019), very few studies have investigated their functional correlates. Recent electrophysiological research reported increased beta-band activity in participants with 15q11.2-q13.1 duplications (Frohlich et al., 2016, 2019) and 16p11.2 deletions (Hinkley et al., 2019), as well as delayed evoked responses in the latter (Berman et al., 2016; Jenkins et al., 2016). Based on current evidence it is difficult to assess the extent of functional connectivity alterations, especially for rarer ND-CNVs.

To address this, we investigated oscillatory connectivity measured with MEG in participants with ND-CNVs at nine different loci. Given the common phenotypic outcomes associated with ND-CNVs (Chawner et al., 2019), this approach can identify convergent endophenotypes of potentially higher clinical relevance. Because a third of our cohort had 22q11.2 deletions, we also investigated alterations in connectivity separately in this subgroup and in the group of participants with other ND-CNVs. This allowed us to assess the specificity of the effects, especially considering previous findings of widespread neural alterations associated with 22q11.2 deletions.

In both subgroups, we found evidence of disrupted alpha and beta-band oscillatory connectivity in posterior brain regions. Furthermore, using graph theory measures of network topology and information transfer, we were able to identify participants with ND-CNVs based on their individual connectivity maps. The two approaches highlighted common patterns of dysconnectivity in participants with ND-CNVs, as well as specific network features that might be linked to CNV pathogenicity.

Methods

Participants

MEG data were acquired in 42 adults with ND-CNVs targeted for their high penetrance for neurodevelopmental disorders (22 female; mean age 38.5±12.5 years). ND-CNVs at nine different loci were represented in the cohort, with 14 (33%) participants carrying 22q11.2 deletions (Table 1).

Recruitment was performed through NHS genetics clinics and relevant support groups within the UK. Written consent was obtained in accordance with The Code of Ethics of the World Medical Association (Declaration of Helsinki), and all procedures were approved by the South East Wales Research Ethics Committee.

All participants with ND-CNVs were assessed using the Psychiatric Assessment Schedule for Adults with Developmental Disability (PAS-ADD; Moss et al., 1997). 24 were also assessed using the Structured Interview for Prodromal Symptoms (SIPS; Miller et al., 2003), and 26 using the Structured Clinical Interview for DSM (SCID II; First and Gibbon, 2004). Diagnoses were assigned by research psychologists and verified by an adult psychiatrist using the Diagnostic and Statistical Manual for Mental Disorders, 4th and 5th Editions. Of the 42 participants, 34 had at least one diagnosis; 22 had anxiety disorders, 15 had mood disorders, and 15 had neurodevelopmental disorders (including 6 with intellectual disability and 6 with

autism spectrum disorders). Five participants exhibited full or attenuated psychotic symptoms, of whom four met the criteria for a psychotic disorder, with two schizophrenia diagnoses in the 22q11.2 deletion group. There was no significant difference in number of diagnoses between the 22q11.2 deletion group and the other ND-CNV group ($t(33.7) = 0.14$, $P = 0.89$).

IQ tests were administered using the Wechsler Adult Intelligence Scale (WAIS-III). We report Verbal IQ (VIQ), Performance IQ (PIQ) and Full Scale IQ scores (FSIQ). There was no significant difference in IQ between the 22q11.2 deletion group and the other ND-CNV group ($t(22.7\text{-}25.1) < 0.57$, $P > 0.58$).

In the ND-CNV group, 62% of participants were taking medication for physical, neurological or mood disorders (e.g. high blood pressure, asthma, pain/migraine, depression/anxiety), with the most common medications including gabapentin, co-codamol (combination of codeine and paracetamol), and fluoxetine (N = 3). Given the high variability of medications, their effects could not be systematically investigated; however, their impact was alleviated in MEG analysis by tests of generalizibility (e.g. resampling).

Controls were selected among resting-state datasets acquired at CUBRIC as part of the "100 Brains"' and "UK MEG Partnership" projects. These cohorts included healthy participants aged 18-65 with no history of neurological or neuropsychiatric disorders, and 42 controls were chosen to match the gender and age of the ND-CNV carriers as closely as possible (22 female; mean age 33.3±9.6 years). These measurements were acquired under protocols approved by the Cardiff University School of Psychology Ethics Committee.

Since a third of the ND-CNV cohort consisted of participants with 22q11.2 deletions, we assessed the impact of this subgroup by repeating all analyses on (1) participants with other ND-CNVs (except 22q11.2 deletions) and their matched controls (N = 56), and (2) participants with 22q11.2 deletions and their matched controls (N = 28).

CNV and critical region (hg19)	Total N	N female	Age (mean±SD)	N diag (mean±SD)	VIQ (mean±SD)	PIQ (mean±SD)	FSIQ (mean±SD)
All CNV	*42*	*22*	*38.53±12.55*	*2.93±2.54*	*88.72±18.84*	*96.63±14.63*	*91.24±17.15*
22q11.2del chr22:19,037,332-21,466,726	14	9	38.97±16.43	3±2.07	86.28±21.23	95.28±15.6	89.93±17.88
22q11.2dup chr22:19,037,332-21,466,726	4	13	38.32±10.44	2.89±2.78	90±17.77	97.33±14.36	91.89±17.08
17q12dup chr17:34,815,904-36,217,432	2						
16p11.2del chr16:29,650,840-30,200,773	1						
16p11.2dup (distal) chr16:28,823,196-29,046,783	1						
15q13.1-13.3del (BP4-5) chr15:31,080,645-32,462,776	2						
15q13.1-13.3dup (BP4-5) chr15:31,080,645-32,462,776	1						
15q11.2del (BP1-2) chr15:22,805,313-23,094,530	7						
15q11.2dup(BP1-2) chr15:22,805,313-23,094,530	1						
15q11.2q12dup(BP2-3; PWS/AS) chr15:22,805,313-28390339	1						
3q29del chr3:195,720,167-197,354,826	1						
2p16.3del (NRXN1) chr2:50145643-51259674	1						
1q21.1del chr1:146,527,987-147,394,444	5						
1q21.1dup chr1:146,527,987-147,394,444	1						
Controls	*42*	*22*	*33.35±9.58*	-	-	-	-

Table 1. Participant information (ND-CNV status, demographic information, number of psychiatric diagnoses, and IQ). Note that the 22q11.2 deletion group included two atypical deletions and one adjacent deletion.

Genotyping

Participants with ND-CNVs were genotyped using the Illumina HumanCoreExome whole genome SNP array, which contained an additional 27 000 genetic variants at loci previously linked to neurodevelopmental disorders, including CNVs. The raw intensity data was

processed using Illumina Genome Studio software (version 2011.1). PennCNV (version 1.0.3) was used to perform CNV calling in order to confirm the presence of the ND-CNV in each case sample, with each CNV being required to span a minimum of 10 informative SNPs and to be at least 10 kb in length. CNV coordinates were specified according to genome version hg19, and the boundaries of each CNV were confirmed by manually inspecting the Log R ratio and B allele frequency plots at each of the genomic regions of interest (Table 1). Genetic information was not available for control participants; given the rarity of these genotypes in the general population, they were assumed to carry no ND-CNVs.

Data collection

Five-minute resting-state MEG recordings were made using a 275-channel CTF radial gradiometer system (CTF, Vancouver, Canada) at a sampling rate of 1200 Hz. Three of the sensors were turned off due to excessive noise, and 29 reference channels were recorded to improve noise cancellation(Vrba, 2002). During the recordings, participants were seated upright and fixated their eyes on a red fixation point presented centrally on either a CRT monitor or LCD projector. Three electromagnetic coils were placed at fiducial locations (nasion and pre-auricular) for head localization.

To aid in source localization, structural T1-weighted MRI scans were also acquired using a 3T General Electric or Siemens MRI scanner with a 1 mm isotropic FSPGR/MPRAGE pulse sequence.

Data analysis

Pre-processing

To remove muscle artifacts, a semi-automatic procedure was implemented using the FieldTrip toolbox (Oostenveld et al., 2011) and MATLAB R2015a. Sensor time-series were bandpass-filtered between 110 and 140 Hz and z-transformed; segments exceeding a participant-specific z-score threshold were removed. Next, eye movement and cardiac artifacts were projected out

of the data using Independent Component Analysis (ICA). Noisy channels exhibiting high variance were also removed from the data where necessary. There was no significant difference in recording duration after artifact rejection between the ND-CNV and control groups ($t(81.8) = 1.61$, $P = 0.11$, mean duration 255.88±29.31 s and 245.33±30.86 s respectively).

Head motion was monitored continuously in 18/42 ND-CNV datasets and 40/42 control datasets, and head localization was performed at the start and end of the recording in the remaining datasets. There was no significant difference between the ND-CNV and control groups in maximum head coil displacement between the beginning and end of the recording ($t(79.8) = 0.85$, $P = 0.39$, mean displacement 2.07±3.62 mm and 2.7±3.06 mm respectively). In datasets with continuous head localization, the maximum distance of the head coils from their average position across the entire recording did not significantly differ between groups ($t(39.4) = 1.44$, $P = 0.16$, mean distance 4.74±3.5 mm and 3.21±4.2 mm respectively).

Prior to source localization, coregistration was performed by manually marking head coil locations on each participant's MRI using FieldTrip. The data were downsampled to 600 Hz and bandpass-filtered in six different frequency bands: delta (2-4 Hz), theta (4-8 Hz), alpha (8-13 Hz), beta (13-30 Hz), low gamma (40-60 Hz), and high gamma (60-90 Hz).

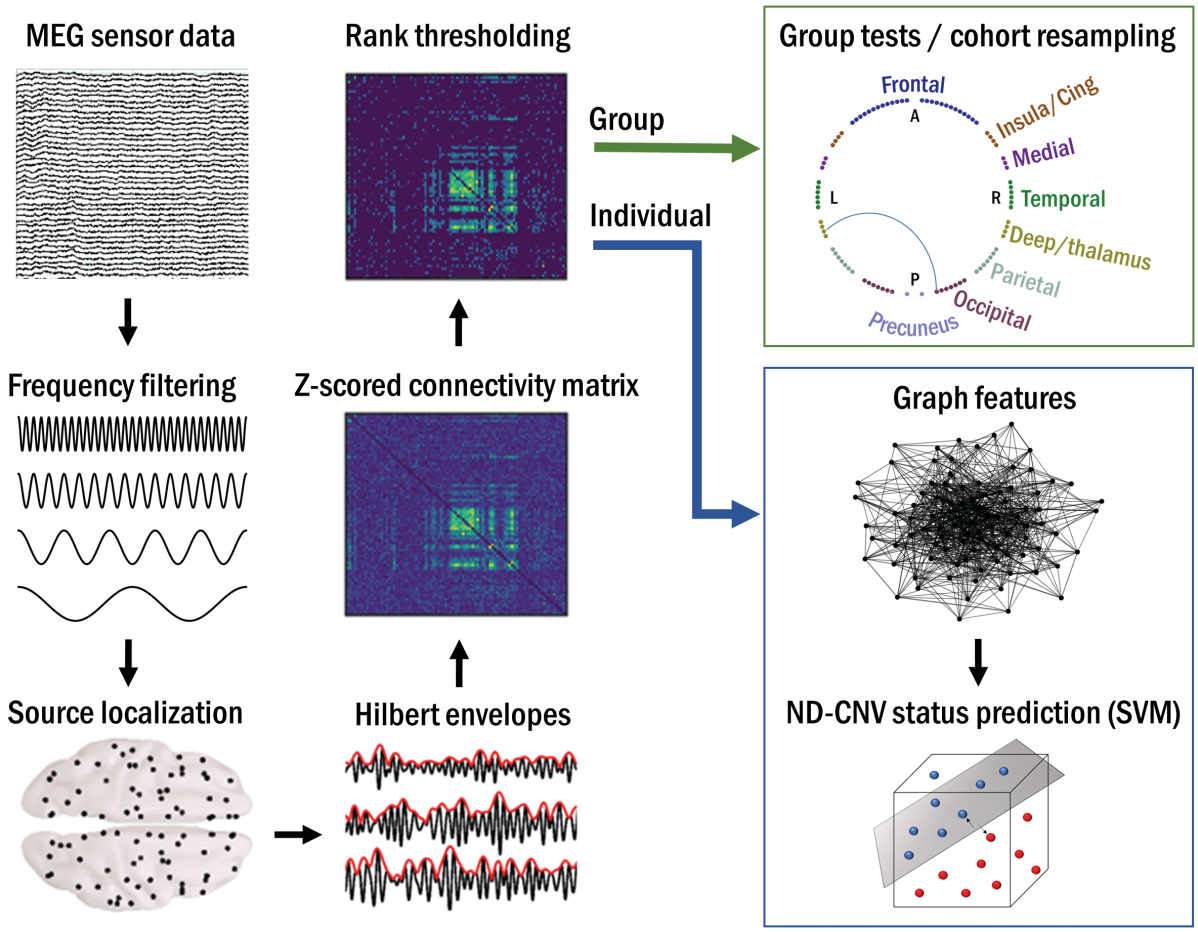

Figure 1. Overview of the analysis pipeline. Resting-state MEG data were preprocessed, filtered into six frequency bands, and projected into source space. Hilbert envelopes were calculated at 90 AAL-atlas-based virtual sensor locations, and correlated to obtain functional connectivity matrices. These were z-scored and rank-thresholded at the group level for between-group analyses, and at the subject level for data-driven prediction of ND-CNV status using graph theory.

Estimating functional connectivity

To assess group differences in resting-state connectivity (Figure 1), we focused on amplitude-amplitude coupling of source-localized oscillatory signals (Colclough et al., 2016). Continuous data in each of the six frequency bands were projected into source space using a Linearly Constrained Minimum Variance (LCMV) beamformer. Sources were reconstructed on a 6 mm template grid warped to each participant's MRI, using a multiple local-spheres forward model (Huang et al., 1999). To alleviate the depth bias, beamformer weights were normalized by their vector norm (Hillebrand et al., 2012).

Next, 90 nodes corresponding to cortical regions of interest (ROI) in the Automated Anatomical Labelling (AAL) atlas (Tzourio-Mazoyer et al., 2002) were identified by performing a frequency analysis on all sources within each ROI and selecting the source with the largest temporal standard deviation. Continuous virtual sensor timecourses corresponding to the 90 nodes were then reconstructed and bandpass-filtered into the frequency bands of interest.

To avoid spurious correlations, the node time-series were orthogonalized using a multivariate symmetric orthogonalization approach (Colclough et al., 2015). A Hilbert transform was used to calculate oscillatory amplitude envelopes, which were then despiked using a median filter, downsampled to 1 Hz, and trimmed to avoid filter and edge effects. To obtain connectivity matrices, pairwise correlations were calculated between the 90 Hilbert envelopes. Next, a Fisher transform was applied to obtain z-scores with zero mean and unit variance across connections in each participant's map. This procedure corrected for possible systematic differences across participants, for example due to differences in data quality (Siems et al., 2016).

Intracranial volume (ICV), quantified as the number of 1-mm isotropic voxels inside the brain, was smaller in the ND-CNV group than the control group ($t(65.5) = -2.19$, $P = 0.03$), in line with some previous reports (Hu et al., 2017; Sønderby et al., 2018; Warland et al., 2019). The potential impact of this difference on the MEG results was alleviated through the source localization procedure and the z-scoring of the connectivity matrices.

In addition to the six frequency bands listed above, a combined measure of connectivity was obtained by calculating the vector-sum of connectivity matrices across all frequency bands (Koelewijn et al., 2019).

Group differences in resting-state connectivity

To reduce the impact of noise, a conservative ranking procedure(Koelewijn et al., 2019) was used to threshold the connectivity maps for the purposes of between-group comparisons. This consisted of calculating the rank of each connection in participant-level connectivity matrices and averaging the resulting rank map across participants in each group. Only the top 20% edges in the average rank map were considered "valid" and selected for further analysis. To ensure that large differences in signal across cohorts were not discarded by this procedure, the rank-thresholding procedure was performed separately in each cohort, and connections determined as "valid" in either cohort were included in further analysis.

To assess differences between groups, Welch's t-tests were conducted at each valid edge. Significant edges were identified using an uncorrected $\alpha = 0.05$. Correction for multiple comparisons was applied using a randomization procedure with 10000 sign-shuffling iterations and maximal statistic thresholding (omnibus $\alpha = 0.05$)(Nichols and Holmes, 2001).

The robustness of cohort differences was evaluated through a resampling procedure. Increases and decreases in connectivity between groups were tabulated using random samples of half of each group. This was repeated across 10000 iterations, and edges showing a consistent effect direction across at least 95% of iterations were considered robust.

To control for potential confounds (for example, resulting from imperfect age matching between the ND-CNV and control groups), an additional multiple regression analysis was performed. Combined-frequency connectivity matrices were entered as response variables with a categorical predictor (ND-CNV presence) and three covariates (age, gender, and ICV). A resampling procedure as described above was performed to assess the robustness of between-group differences. The sign of the regression slope associated with the main predictor was tabulated across 1000 split-half cohort randomizations. Edges showing consistent effects across 95% of iterations were considered robust.

207 **Individual networks: identifying participants with ND-CNVs using graph theory**

208 Next, a data-driven graph theory approach was used to assess whether participants with ND-
209 CNVs could be distinguished from unaffected controls using functional connectivity features.
210 To this aim, the cohort was divided into training and test sets using an iterated cross-validation
211 procedure.

212 This analysis focused on individual networks by selecting the top 20% of connections in each
213 participant's normalized connectivity map as the basis for undirected graphs. Networks were
214 then characterized using six nodal graph theory metrics. These included three measures of node
215 connectedness: *degree* (the number of connections linking each node to other nodes);
216 *betweenness centrality* (the fraction of shortest paths between nodes containing a given node);
217 and *eccentricity* (the maximal shortest path from a node to any other node). *Global efficiency*
218 (the average inverse shortest path between a node and all others) was evaluated as a measure
219 of network integration. Finally, two metrics captured network modularity: *local efficiency* (the
220 average inverse shortest path between a node and its neighbours) and *clustering coefficient* (the
221 fraction of connected node triplets around a node). All metrics with the exception of node
222 degrees were weighted by the inverse of the normalized connectivity matrices; in other words,
223 stronger amplitude-amplitude coupling was taken to reflect shorter paths between nodes. Graph
224 theory analyses were performed using MATLAB R2019a and the Brain Connectivity Toolbox
225 (Rubinov and Sporns, 2010).

226 To discriminate between groups, a linear support vector machine (SVM) classifier (Boser et
227 al., 1992) was trained on each of the node metrics. Additionally, a pooled feature vector was
228 created by combining the six metrics to maximize the amount of complementary information
229 input to the classifier. This approach makes use of information across all nodes while avoiding
230 the need for multiple testing.

231 Classification was performed between the ND-CNV and control groups, as well as between the
232 two ND-CNV subgroups (22q11.2 deletions and other ND-CNVs) and their matched controls.
233 To avoid overfitting, model performance was evaluated using 100 iterations of stratified five-
234 fold cross-validation. This entailed iteratively leaving out a fifth of the data for testing and
235 training the model on the remaining data, whilst ensuring balanced group representation in each
236 fold. Performance was quantified using accuracy (proportion correctly classified observations),
237 sensitivity (true positive rate) and specificity (true negative rate) in order to highlight any
238 asymmetries in ND-CNV and control identification. Furthermore, significance was assessed
239 by shuffling the true labels 5000 times and recomputing classifier accuracy to estimate the
240 empirical chance level and calculate a one-tailed p-value (Nichols and Holmes, 2001).

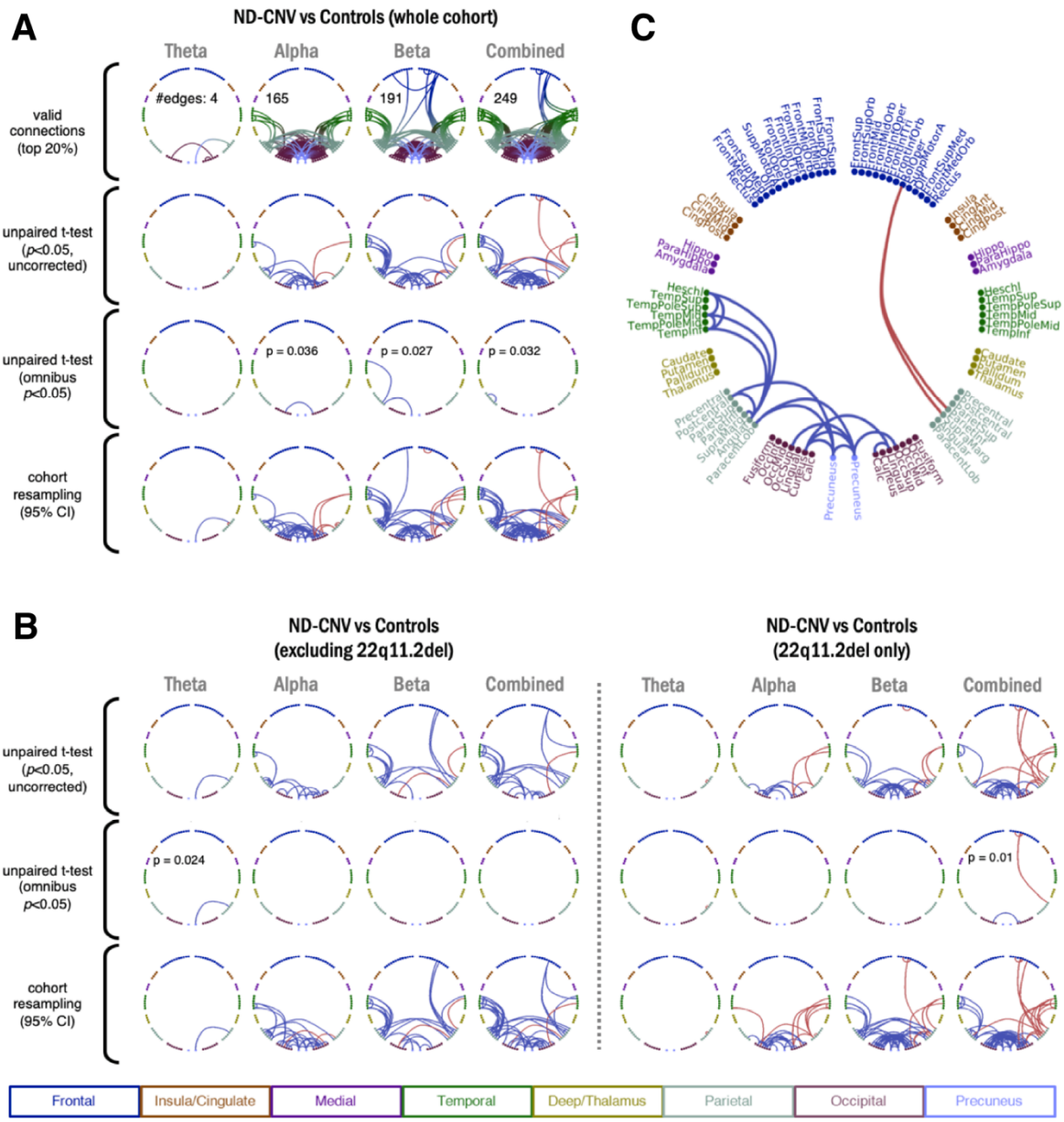

Figure 2. A. Differences in resting-state connectivity (amplitude correlations) between participants with ND-CNVs and controls. Connectivity increases and decreases in the ND-CNV group are shown in red and blue respectively. The rows show (top to bottom): valid connections after mean-rank thresholding in each frequency band; uncorrected (P<0.05) differences between groups; multiple comparison-corrected (omnibus P<0.05) differences between groups; and connections showing consistent increases/decreases in 95% of cohort resampling iterations. **B.** As in A, for subgroups excluding participants with 22q11.2 deletions and their matched controls (left) or including only participants with 22q11.2 deletions and their matched controls (right). To facilitate comparison, "valid" connections were the same as in A. Only frequency bands with surviving "valid" connections are shown. **C.** Nodes displayed in the circular plots, labelled and colour-coded by region. Connections shown are

the result of the conjunction analysis between the 22q11.2 deletion group and the other ND-CNV group (also see Figure 3: blue connections are decreased in both groups; red connections have opposing signs).

Results

Connectivity alterations associated with ND-CNVs

The analysis of group differences in oscillatory connectivity revealed the largest number of valid connections in the alpha and beta bands (Figure 2). Most of the significantly different connections showed a decrease in oscillatory connectivity between posterior, parietal and temporal nodes in the ND-CNV group, with the exception of a few right-hemisphere edges. More extensive cohort effects were detected using the combined frequency maps (61 edges exceeded the uncorrected threshold, compared to 1, 28 and 42 in the theta, alpha and beta bands). These patterns were robust to random sub-sampling of the cohort, suggesting that they were not driven by individual subjects. A small number of left-hemisphere connections, including the precuneus, early visual cortex, and parietal regions, survived omnibus correction for multiple comparisons.

Importantly, a similar pattern of hypoconnectivity was observed even after excluding participants with 22q11.2 deletions and their matched controls (Figure 2B-C). Both ND-CNV subgroups showed decreased posterior connectivity (Figure 3; 18 connections decreased in both groups), indicating that the overall pattern was not driven by the 22q11.2 deletion group. This pattern occurred despite higher heterogeneity in the mixed ND-CNV group (Figure 4) and might thus reflect convergent alterations across genotypes. On the other hand, participants with 22q11.2 deletions exhibited more right-hemisphere hyperconnectivity compared to controls. These effects spanned the precuneus and parietal cortex, as well as frontal regions, suggesting some overlap with the default mode network (DMN).

To ensure that these differences were not affected by potential confounds, the cohort resampling tests on combined frequency maps were repeated as a multiple linear regression with age, gender and ICV as covariates. This analysis revealed fewer connections (65 compared to the original 92 in the whole cohort analysis), but largely similar patterns of dysconnectivity (Figure 3B).

Furthermore, although IQ scores could not be included in this analysis because they were not available for the control group, IQ scores in the ND-CNV group significantly correlated with connectivity strength at only four edges (max Pearson's $r = 0.5$, $P<0.05$).

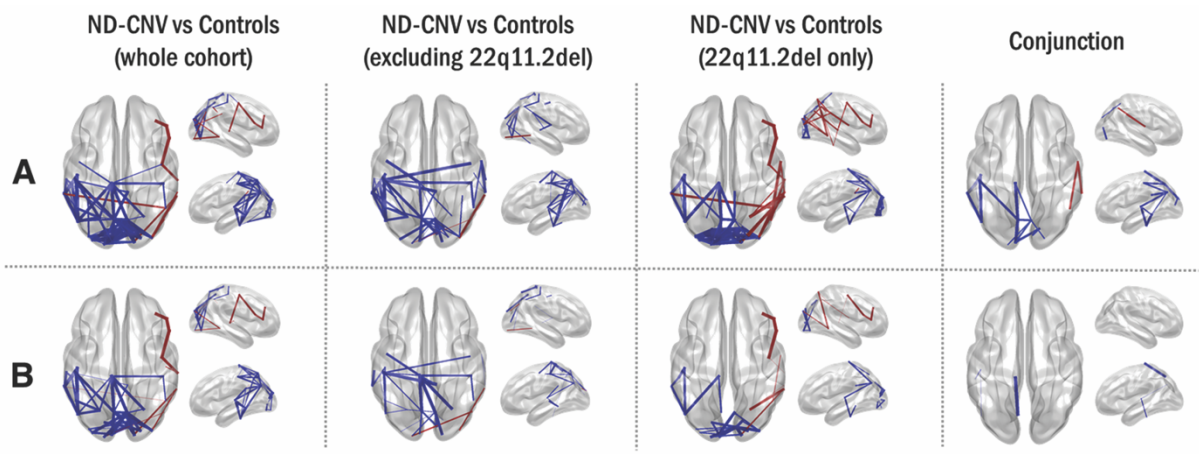

Figure 3. Differences in connectivity are not driven by age, gender, and intracranial volume. Connections meeting the 95% confidence criterion in the cohort resampling test are displayed for all group tests (first three columns). The last column shows supra-threshold connections in both the 22q11.2 deletion group and the other ND-CNV group; they are shown in blue where they are decreased in both groups, and in red where they have opposite signs. Line width increases with effect robustness. **A**. Connections exhibiting robust differences based on the cohort resampling test of combined frequency matrices, plotted on the template brain. **B.** As in A, after including age, gender and intracranial volume as covariates in a multiple linear regression with "ND-CNV presence" as a main categorical predictor.

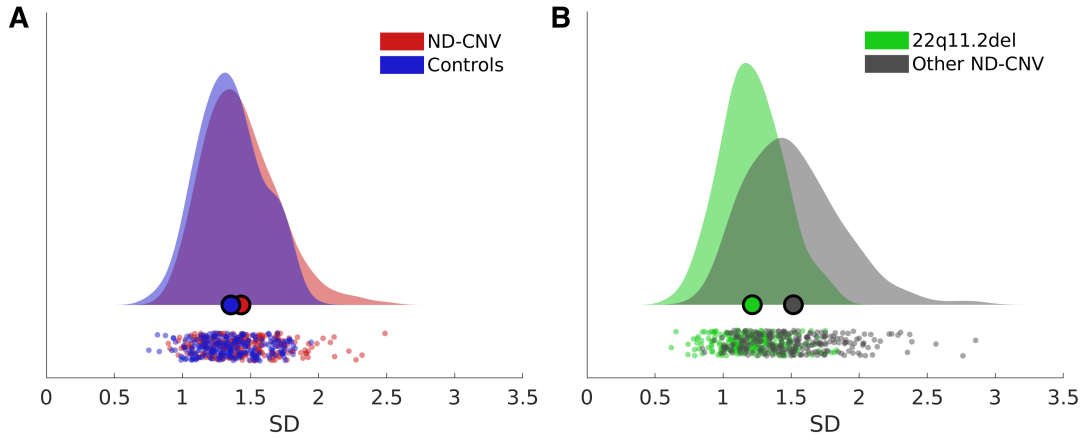

Figure 4. Variability in connection z-scores across participant groups. The distribution of standard deviations (SD) across valid connections in the combined frequency maps are shown for: **A.** the ND-CNV and control groups; **B.** the two ND-CNV subgroups. The mixed ND-CNV group displays larger variability. Plots were generated using the RainCloudPlots toolbox (Allen et al., 2019).

Network features as predictors of ND-CNV status

A graph theory framework was employed to identify participants with ND-CNVs from their functional networks based on combined frequency maps. This approach has the advantage of reducing dimensionality and complements the edge-focused group testing approach described above.

Graph theory metrics were successful predictors of ND-CNV participants relative to unaffected controls. The best prediction accuracy was achieved by combining the 6 node features (Table 2; Figure 5A; maximum accuracy 71%±3.44, P=0.0002). However, participants with 22q11.2 deletions were more consistently correctly classified than those with other ND-CNVs (Figure 5B).

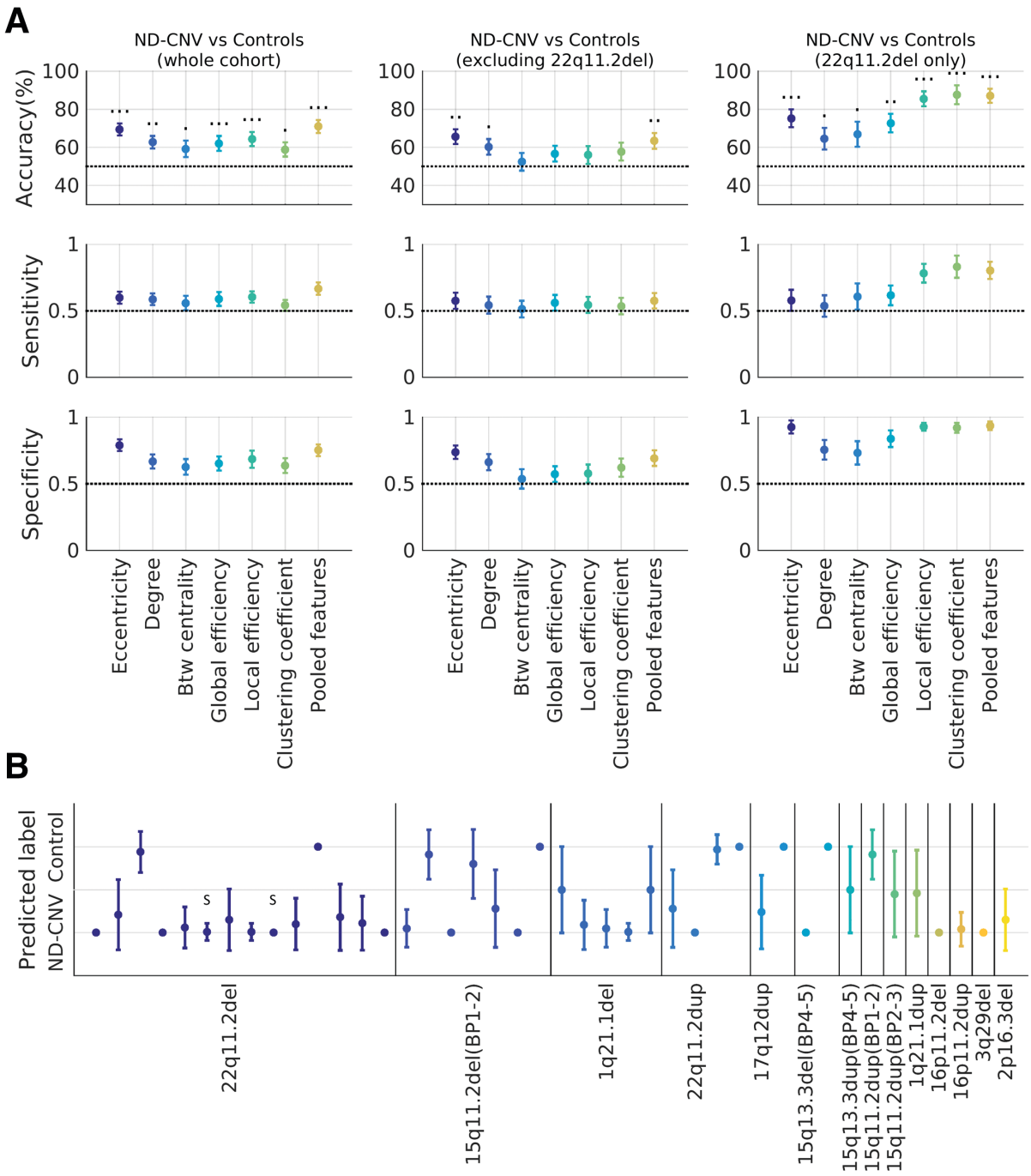

Figure 5. Classifying participants with ND-CNVs and unaffected controls from individual MEG functional networks using graph theory. **A:** Classification performance on the three groups, using different metrics to characterize the networks (eccentricity, degree, betweenness centrality, global and local efficiency, clustering coefficient, and the pooled model). Above-chance accuracies (permutation testing) are marked with 1, 2, and 3 dots respectively for $p<0.05$, $p<0.01$, and $p<0.001$. **B.** How well are different ND-CNVs classified? The plot shows the mean predicted label for each of the 42 participants with ND-CNVs across 100 cross-validation iterations using pooled node features. Participants with 22q11.2 deletions are most consistently correctly identified. Two participants with schizophrenia diagnoses are marked with "S".

315 This was confirmed by subgroup classification analyses, which also pointed to subgroup
316 differences. When excluding participants with 22q11.2 deletions, the best decoding accuracies
317 were achieved using node eccentricities (65.62%±3.91, *P*=0.0016), node degrees, and the joint
318 feature model. On the other hand, all node features were successful in discriminating
319 participants with 22q11.2 deletions from their matched controls, with the best performance
320 obtained using the clustering coefficient (87.61%±4.95, *P*=0.0002).

321 These results point to commonalities in network features (such as decreased centrality) that
322 allow for the successful classification of participants with ND-CNVs across distinct genotypes.
323 On the other hand, the features are specific enough to allow successful discrimination between
324 participants with 22q11.2 deletions and other ND-CNVs (Table 2). Given the higher overall
325 burden of 22q11.2 deletions in neurodevelopmental disorders (Kirov et al., 2014), this suggests
326 that increased neurodevelopmental risk may be associated with more salient alterations in
327 network function and may underpin specific genotype effects.

	ND-CNV vs Controls (whole cohort)							**22q11.2del vs other ND-CNV**
	Eccentricity	*Degree*	*Betweenness centrality*	*Global efficiency*	*Local efficiency*	*Clustering coefficient*	*Pooled node features*	*Pooled node features*
Accuracy (%)	69.41	62.74	59.25	62.1	64.44	58.9	71	72.43
SD	3.14	3.25	4.3	3.91	3.7	3.72	3.44	1.63
P-value	0.0002	0.0012	0.0108	0.001	0.0006	0.022	0.0002	0.0036
Sensitivity	0.6	0.59	0.56	0.59	0.6	0.54	0.67	0.67
Specificity	0.79	0.67	0.63	0.65	0.68	0.64	0.75	0.75
	ND-CNV vs Controls (excluding 22q11.2del and matched controls)							**Train on 22q11.2del, test on other ND-CNV**
Accuracy (%)	65.62	60.27	52.45	56.69	56.06	57.82	63.43	55.36
SD	3.91	4.12	4.65	4.14	4.7	4.72	4.16	-
P-value	0.0016	0.0242	0.2967	0.1038	0.1032	0.053	0.0068	0.225
Sensitivity	0.58	0.54	0.51	0.56	0.55	0.53	0.58	0.21
Specificity	0.74	0.66	0.54	0.57	0.58	0.62	0.69	0.89
	ND-CNV vs Controls (22q11.2del vs matched controls only)							**Train on other ND-CNV, test on 22q11.2del**
Accuracy (%)	75.31	64.56	66.91	72.75	85.53	87.61	87.07	75
SD	4.7	5.69	6.52	4.89	3.94	4.95	3.69	-
P-value	0.0002	0.0296	0.0118	0.003	0.0002	0.0002	0.0002	0.0048
Sensitivity	0.58	0.54	0.61	0.62	0.78	0.83	0.8	0.57
Specificity	0.93	0.75	0.73	0.84	0.93	0.92	0.94	0.93

328

329 **Table 2**. Network-based classification results. Note that cross-decoding across ND-CNV subgroups achieves high
330 specificity but not sensitivity (middle-right and lower-right cells). This suggests that classifier performance is
331 driven mainly by network features in the control group.

332 For classification between participants with 22q11.2 deletions and other ND-CNVs (top right cell), 100 subsamples
333 of 14 participants were drawn from the 28 carriers of other ND-CNVs, gender-matched to the 22q11.2 deletion
334 group. The subgroups were similar in age, ensuring balanced classes in terms of sample size, gender, and age.
335 Predicted labels were then averaged across cohort resamplings (mean 50±5.57 repetitions per participant).

336 Discussion

337 To our knowledge, the present study provides the first insight into oscillatory connectivity
338 alterations in people with rare ND-CNVs. Using both an established group analysis pipeline
339 and a data-driven graph theory framework, we uncovered a pattern of functional
340 dysconnectivity affecting posterior regions in participants with ND-CNVs. These patterns were
341 robust to effects of age, gender, and intracranial volume, and emerged despite a conservative
342 thresholding approach restricted to the most reproducible connections.

343 Effects originated in the alpha and beta frequency bands, which are thought to underpin long-
344 range communication between brain areas (Schnitzler and Gross, 2005). Connections linking
345 parietal, temporal, and occipital areas were most consistently affected in both the 22q11.2
346 deletion group and the other ND-CNV group. Similar patterns have been previously reported
347 in schizophrenia patients (Brookes et al., 2016), including alpha-band parietal
348 hypoconnectivity in first-episode schizophrenia (Phalen et al., 2019). Furthermore, posterior
349 structural network alterations have been identified as an early marker of ASD (Lewis et al.,
350 2014), suggesting a link between such alterations and increased neurodevelopmental risk.

351 Similar connectivity changes in the visual processing system and the default mode network
352 have been shown in people with 22q11.2 deletions using structural and functional MRI
353 (Schreiner et al., 2014; Scariati et al., 2016a; Larsen et al., 2019). Here, we found that these

354 effects are not restricted to the 22q11.2 deletion group, suggesting that long-range connectivity
355 could act as a common marker across genetic variants. Although non-invasive measurements
356 cannot provide direct mechanistic insight, this is consistent with potential alterations in
357 excitatory-inhibitory balance (Deco et al., 2014; Gu et al., 2019) as a mechanism for pleiotropic
358 genetic effects underlying neurodevelopmental disorders (Gao and Penzes, 2015; Foss-Feig et
359 al., 2017; Lee et al., 2017). This is thought to occur through increased excitation or disinhibition
360 caused by gene haploinsufficiency and mediated by impaired GABA and NMDA receptor
361 function (Kehrer et al., 2008; Ramamoorthi and Lin, 2011; Pocklington et al., 2015).

362 Despite sample size limitations, differences between the two subgroups also point to effects
363 specific to the highly penetrant 22q11.2 deletions. Hypoconnectivity was more extensive in
364 people with other ND-CNVs, while the 22q11.2 deletion group exhibited more focused
365 patterns; these were robust to cohort resampling, suggesting that they are unlikely to be driven
366 by individual cases. These differences were reflected in the graph theory analysis. Although all
367 network features were altered in the 22q11.2 deletion group, their increased modularity was
368 particularly discriminative, in line with previous reports of increased structural network
369 segregation in people with 22q11.2 deletions (Ottet et al., 2013; Scariati et al., 2016b; Sandini
370 et al., 2018). For other ND-CNVs, the only predictive features were centrality measures
371 (specifically the node eccentricity and degree), reflecting hypoconnectivity in the ND-CNV
372 cohort. Between and within-group classification results (Table 2) highlight the ability of graph
373 theory metrics to capture both convergent and specific network alterations, which could help
374 elucidate the link between CNV pathogenicity and neural system function.

375 We alleviated concerns of potential systematic between-group differences unrelated to
376 genotype by using conservative approaches (e.g. rejecting weaker connections that may
377 introduce noise) and resampling procedures. Although head motion did not appear to differ

between groups, this was not continuously measured in all participants and so we could only partially rule out its effects.

Although the present study was able to evaluate ND-CNV effects independently of the contribution of highly penetrant 22q11.2 deletions, the limited sample size remains a concern common in CNV imaging research. The high genotype variability within the cohort makes the specificity of these effects difficult to assess, particularly with regard to differences between the 22q11.2 deletion group and other ND-CNVs. Variability within the heterogeneous ND-CNV group was higher than within the 22q11.2 deletion group (Figure 4), suggesting that our focus on convergent alterations may obscure specific effects. However, the fact that we see differences robust to resampling in this group, despite its heterogeneity, points to common connectivity alterations across distinct genotypes. Studies recruiting larger samples of participants with ND-CNVs, for example through large multi-site collaborations, are necessary to evaluate the generalizability of connectivity patterns and graph theory metrics as "fingerprints" associated with ND-CNV status.

In summary, the present study assessed oscillatory long-range connectivity as a potential marker of pathogenic genetic effects across a range of rare ND-CNVs. Occipital, parietal and temporal brain areas were characterized by consistent hypoconnectivity across genotypes, which was not exclusively driven by the presence of a large number of participants with highly-penetrant 22q11.2 deletions. Functional networks in the ND-CNV group exhibited decreased node centrality and alterations in network efficiency and structure. Furthermore, features specific to highly penetrant variants were present alongside convergent network alterations and enabled successful ND-CNV classification. These results are consistent with a common mechanism for genetic risk, based on an altered balance between excitatory and inhibitory synaptic processes and leading to network dysfunction. We propose that these functional

connectivity alterations are an intermediate phenotype on the pathway from synaptic molecular changes to disruption of cognitive function and psychotic illness.

Conflict of interest

The authors declare no competing interests.

Acknowledgements

The authors wish to thank: Ffion Evans and Kali Barawi for assistance with psychometric and clinical data collection; Eirini Messaritaki for helpful comments on the graph theory analysis; George Kirov for help with genetic data; and Alexander Shaw for the SourceMesh visualization toolbox. This work was supported by a Wellcome Trust Strategic Award (100202/Z/12/Z), the MRC UK MEG Partnership Grant (MR/K005464/1), and the MRC Doctoral Training Grant (MR/K501086/1).

References

Allen M, Poggiali D, Whitaker K, Marshall TR, Kievit RA (2019) Raincloud plots: A multi-platform tool for robust data visualization [version 1; peer review: 2 approved]. Wellcome Open Res 4.

Berman JI, Chudnovskaya D, Blaskey L, Kuschner E, Mukherjee P, Buckner R, Nagarajan S, Chung WK, Sherr EH, Roberts TPL (2016) Relationship between M100 Auditory Evoked Response and Auditory Radiation Microstructure in 16p11.2 Deletion and Duplication Carriers. AJNR Am J Neuroradiol 37:1178–1184.

Boot E, van Amelsvoort TAMJ (2013) Neuroimaging Correlates of 22q11.2 Deletion Syndrome: Implications for Schizophrenia Research. Curr Top Med Chem 12:2303–2313.

Boser BE, Guyon IM, Vapnik VN (1992) A training algorithm for optimal margin classifiers. In: Proceedings of the fifth annual workshop on Computational learning theory - COLT '92, pp

144–152. New York, New York, USA: ACM Press.

Brookes MJ, Tewarie PK, Hunt BAE, Robson SE, Gascoyne LE, Liddle EB, Liddle PF, Morris PG (2016) A multi-layer network approach to MEG connectivity analysis. Neuroimage 132:425–438.

Chawner SJRA, Owen MJ, Holmans P, Raymond FL, Skuse D, Hall J, van den Bree MBM (2019) Genotype-phenotype associations in children with copy number variants associated with high neuropsychiatric risk in the UK (IMAGINE-ID): a case-control cohort study. The Lancet Psychiatry 6:493–505.

Colclough GL, Brookes MJ, Smith SM, Woolrich MW (2015) A symmetric multivariate leakage correction for MEG connectomes. Neuroimage 117:439–448.

Colclough GL, Woolrich MW, Tewarie PK, Brookes MJ, Quinn AJ, Smith SM (2016) How reliable are MEG resting-state connectivity metrics ? Neuroimage 138:284–293.

Debbané M, Lazouret M, Lagioia A, Schneider M, Van De Ville D, Eliez S (2012) Resting-state networks in adolescents with 22q11.2 deletion syndrome: Associations with prodromal symptoms and executive functions. Schizophr Res 139:33–39.

Deco G, Ponce-Alvarez A, Hagmann P, Romani GL, Mantini D, Corbetta M (2014) How local excitation-inhibition ratio impacts the whole brain dynamics. J Neurosci 34:7886–7898.

Dong D, Wang Y, Chang X, Luo C, Yao D (2018) Dysfunction of Large-Scale Brain Networks in Schizophrenia: A Meta-analysis of Resting-State Functional Connectivity. Schizophr Bull 44:168–181.

Drakesmith M, Parker GD, Smith J, Linden SC, Rees E, Williams N, Owen MJ, van den Bree M, Hall J, Jones DK, Linden DEJ (2019) Genetic risk for schizophrenia and developmental delay is associated with shape and microstructure of midline white-matter structures. Transl Psychiatry 9:102.

First MB, Gibbon M (2004) The Structured Clinical Interview for DSM-IV Axis I Disorders (SCID-I)

449 and the Structured Clinical Interview for DSM-IV Axis II Disorders (SCID-II). In:
450 Comprehensive handbook of psychological assessment, Vol. 2. Personality assessment
451 (Hilsenroth MJ, Segal DL, eds), pp 134–143. Hoboken, NJ, US: John Wiley & Sons Inc.

452 Foss-Feig JH, Adkinson BD, Ji JL, Yang G, Srihari VH, McPartland JC, Krystal JH, Murray JD,
453 Anticevic A (2017) Searching for Cross-Diagnostic Convergence: Neural Mechanisms
454 Governing Excitation and Inhibition Balance in Schizophrenia and Autism Spectrum Disorders.
455 Biol Psychiatry 81:848–861.

456 Friston K, Brown HR, Siemerkus J, Stephan KE (2016) The dysconnection hypothesis (2016).
457 Schizophr Res 176:83–94.

458 Frohlich J, Reiter LT, Saravanapandian V, DiStefano C, Huberty S, Hyde C, Chamberlain S, Bearden
459 CE, Golshani P, Irimia A, Olsen RW, Hipp JF, Jeste SS (2019) Mechanisms underlying the EEG
460 biomarker in Dup15q syndrome. Mol Autism 10:29.

461 Frohlich J, Senturk D, Saravanapandian V, Golshani P, Reiter LT, Sankar R, Thibert RL, DiStefano
462 C, Huberty S, Cook EH, Jeste SS (2016) A Quantitative Electrophysiological Biomarker of
463 Duplication 15q11.2-q13.1 Syndrome Ravel N, ed. PLoS One 11:e0167179.

464 Gao R, Penzes P (2015) Common mechanisms of excitatory and inhibitory imbalance in
465 schizophrenia and autism spectrum disorders. Curr Mol Med 15:146–167.

466 Gu H, Hu Y, Chen X, He Y, Yang Y (2019) Regional excitation-inhibition balance predicts default-
467 mode network deactivation via functional connectivity. Neuroimage 185:388–397.

468 Hillebrand A, Barnes GR, Bosboom JL, Berendse HW, Stam CJ (2012) Frequency-dependent
469 functional connectivity within resting-state networks : An atlas-based MEG beamformer
470 solution. Neuroimage 59:3909–3921.

471 Hinkley LBN, Dale C, Luks TL, Findlay AM, Bukshpun P, Pojman N, Thieu T, Chung WK, Berman
472 J, Roberts TPL, Mukherjee P, Sherr EH, Nagarajan SS (2019) Sensorimotor cortical oscillations
473 during movement preparation in 16p11.2 deletion carriers. J Neurosci:3001–3017.

474 Hu M-L, Zong X-F, Mann JJ, Zheng J-J, Liao Y-H, Li Z-C, He Y, Chen X-G, Tang J-S (2017) A
475 Review of the Functional and Anatomical Default Mode Network in Schizophrenia. Neurosci
476 Bull 33:73–84.

477 Huang MX, Mosher JC, Leahy RM (1999) A sensor-weighted overlapping-sphere head model and
478 exhaustive head model comparison for MEG. Phys Med Biol 44:423–440.

479 Hull J V., Dokovna LB, Jacokes ZJ, Torgerson CM, Irimia A, Van Horn JD (2017) Resting-State
480 Functional Connectivity in Autism Spectrum Disorders: A Review. Front Psychiatry 7:205.

481 Jenkins J, Chow V, Blaskey L, Kuschner E, Qasmieh S, Gaetz L, Edgar JC, Mukherjee P, Buckner R,
482 Nagarajan SS, Chung WK, Spiro JE, Sherr EH, Berman JI, Roberts TPL (2016) Auditory
483 Evoked M100 Response Latency is Delayed in Children with 16p11.2 Deletion but not 16p11.2
484 Duplication. Cereb Cortex 26:1957–1964.

485 Jonas RK, Montojo CA, Bearden CE (2014) The 22q11.2 deletion syndrome as a window into
486 complex neuropsychiatric disorders over the lifespan. Biol Psychiatry 75:351–360.

487 Karayiorgou M, Simon TJ, Gogos JA (2010) 22q11.2 microdeletions: linking DNA structural
488 variation to brain dysfunction and schizophrenia. Nat Rev Neurosci 11:402–416.

489 Kehrer C, Maziashvili N, Dugladze T, Gloveli T (2008) Altered excitatory-inhibitory balance in the
490 NMDA-hypofunction model of schizophrenia. Front Mol Neurosci 1:6.

491 Kirov G, Rees E, Walters JTR, Escott-Price V, Georgieva L, Richards AL, Chambert KD, Davies G,
492 Legge SE, Moran JL, McCarroll SA, Donovan MCO, Owen MJ (2014) The penetrance of copy
493 number variations for schizophrenia and developmental delay. Biol Psychiatry 75:378–385.

494 Koelewijn L, Lancaster TM, Linden D, Dima DC, Routley BC, Magazzini L, Barawi K, Brindley L,
495 Adams R, Tansey KE, Bompas A, Tales A, Bayer A, Singh K (2019) Oscillatory hyperactivity
496 and hyperconnectivity in young APOE-ε4 carriers and hypoconnectivity in Alzheimer's disease.
497 Elife 8:1–25.

498 Larsen KM, Dzafic I, Siebner HR, Garrido MI (2019) Alteration of functional brain architecture in

499 22q11.2 deletion syndrome – Insights into susceptibility for psychosis. Neuroimage 190:154–
500 171.

501 Lee E, Lee J, Kim E (2017) Excitation/Inhibition Imbalance in Animal Models of Autism Spectrum
502 Disorders. Biol Psychiatry 81:838–847.

503 Lewis JD, Evans AC, Pruett JR, Botteron K, Zwaigenbaum L, Estes A, Gerig G, Collins L,
504 Kostopoulos P, McKinstry R, Dager S, Paterson S, Schultz RT, Styner M, Hazlett H, Piven J
505 (2014) Network inefficiencies in autism spectrum disorder at 24 months. Transl Psychiatry
506 4:e388–e388.

507 Miller TJ, McGlashan TH, Rosen JL, Cadenhead K, Ventura J, McFarlane W, Perkins DO, Pearlson
508 QD, Woods SW (2003) Prodromal Assessment With the Structured Interview for Prodromal
509 Syndromes and the Scale of Prodromal Symptoms: Predictive Validity, Interrater Reliability,
510 and Training to Reliability. Schizophr Bull 29:703–715.

511 Moss S, Ibbotson B, Prosser H, Goldberg D, Patel P, Simpson N (1997) Validity of the PAS-ADD for
512 detecting psychiatric symptoms in adults with learning disability (mental retardation). Soc
513 Psychiatry Psychiatr Epidemiol 32:344–354.

514 Niarchou M, Chawner SJRA, Doherty JL, Maillard AM, Jacquemont S, Chung WK, Green-Snyder L,
515 Bernier RA, Goin-Kochel RP, Hanson E, Linden DEJ, Linden SC, Raymond FL, Skuse D, Hall
516 J, Owen MJ, Bree MBM van den (2019) Psychiatric disorders in children with 16p11.2 deletion
517 and duplication. Transl Psychiatry 9:8.

518 Niarchou M, Zammit S, van Goozen SHM, Thapar A, Tierling HM, Owen MJ, van den Bree MBM
519 (2014) Psychopathology and cognition in children with 22q11.2 deletion syndrome. Br J
520 Psychiatry 204:46–54.

521 Nichols TE, Holmes AP (2001) Nonparametric Permutation Tests For Functional Neuroimaging : A
522 Primer with Examples. Hum Brain Mapp 25:1–25.

523 O'Reilly C, Lewis JD, Elsabbagh M (2017) Is functional brain connectivity atypical in autism? A

systematic review of EEG and MEG studies Gozzi A, ed. PLoS One 12:e0175870.

Oostenveld R, Fries P, Maris E, Schoffelen JM (2011) FieldTrip: Open source software for advanced analysis of MEG, EEG, and invasive electrophysiological data. Comput Intell Neurosci 2011:156869.

Ottet M-C, Schaer M, Debbané M, Cammoun L, Thiran J-P, Eliez S (2013) Graph theory reveals dysconnected hubs in 22q11DS and altered nodal efficiency in patients with hallucinations. Front Hum Neurosci 7:402.

Owen MJ, Doherty JL (2016) What can we learn from the high rates of schizophrenia in people with 22q11.2 deletion syndrome? World Psychiatry 15:23–25.

Padula MC, Schaer M, Scariati E, Schneider M, Van De Ville D, Debbané M, Eliez S (2015) Structural and functional connectivity in the default mode network in 22q11.2 deletion syndrome. J Neurodev Disord 7:23.

Phalen H, Coffman BA, Ghuman A, Sejdić E, Salisbury DF (2019) Non-Negative Matrix Factorization Reveals Resting-State Cortical Alpha Network Abnormalities in the First Episode Schizophrenia-Spectrum. Biol Psychiatry Cogn Neurosci Neuroimaging.

Pocklington AJ, Rees E, Walters JTR, Han J, Kavanagh DH, Chambert KD, Holmans P, Moran JL, McCarroll SA, Kirov G, O'Donovan MC, Owen MJ (2015) Novel Findings from CNVs Implicate Inhibitory and Excitatory Signaling Complexes in Schizophrenia. Neuron 86:1203–1214.

Ramamoorthi K, Lin Y (2011) The contribution of GABAergic dysfunction to neurodevelopmental disorders. Trends Mol Med 17:452–462.

Reddaway JT, Doherty JL, Lancaster T, Linden D, Walters JT, Hall J (2018) Genomic and Imaging Biomarkers in Schizophrenia. Curr Top Behav Neurosci 40:325–352.

Rubinov M, Sporns O (2010) Complex network measures of brain connectivity: Uses and interpretations. Neuroimage 52:1059–1069.

549 Sandini C, Scariati E, Padula MC, Schneider M, Schaer M, Van De Ville D, Eliez S (2018) Cortical
550 Dysconnectivity Measured by Structural Covariance Is Associated With the Presence of
551 Psychotic Symptoms in 22q11.2 Deletion Syndrome. Biol Psychiatry Cogn Neurosci
552 Neuroimaging 3:433–442.

553 Scariati E, Padula MC, Schaer M, Eliez S (2016a) Long-range dysconnectivity in frontal and midline
554 structures is associated to psychosis in 22q11.2 deletion syndrome. J Neural Transm 123:823–
555 839.

556 Scariati E, Schaer M, Karahanoglu I, Schneider M, Richiardi J, Debbané M, Van De Ville D, Eliez S
557 (2016b) Large-scale functional network reorganization in 22q11.2 deletion syndrome revealed
558 by modularity analysis. Cortex 82:86–99.

559 Schneider M et al. (2014) Psychiatric Disorders From Childhood to Adulthood in 22q11.2 Deletion
560 Syndrome: Results From the International Consortium on Brain and Behavior in 22q11.2
561 Deletion Syndrome. Am J Psychiatry 171:627–639.

562 Schnitzler A, Gross J (2005) Normal and pathological oscillatory communication in the brain. Nat
563 Rev Neurosci 6:285–296.

564 Schreiner MJ, Karlsgodt KH, Uddin LQ, Chow C, Congdon E, Jalbrzikowski M, Bearden CE (2014)
565 Default mode network connectivity and reciprocal social behavior in 22q11.2 deletion
566 syndrome. Soc Cogn Affect Neurosci 9:1261–1267.

567 Sha Z, Wager TD, Mechelli A, He Y (2019) Common Dysfunction of Large-Scale Neurocognitive
568 Networks Across Psychiatric Disorders. Biol Psychiatry 85:379–388.

569 Siems M, Pape A-A, Hipp JF, Siegel M (2016) Measuring the cortical correlation structure of
570 spontaneous oscillatory activity with EEG and MEG. Neuroimage 129:345–355.

571 Silva AI, Ulfarsson MO, Stefansson H, Gustafsson O, Walters GB, Linden DEJ, Wilkinson LS,
572 Drakesmith M, Owen MJ, Hall J, Stefansson K (2019) Reciprocal White Matter Changes
573 Associated With Copy Number Variation at 15q11.2 BP1-BP2: A Diffusion Tensor Imaging

Study. Biol Psychiatry 85:563–572.

Sønderby IE et al. (2018) Dose response of the 16p11.2 distal copy number variant on intracranial volume and basal ganglia. Mol Psychiatry.

Sun D et al. (2018) Large-scale mapping of cortical alterations in 22q11.2 deletion syndrome: Convergence with idiopathic psychosis and effects of deletion size. Mol Psychiatry:1–13.

Tomescu MI, Rihs TA, Becker R, Britz J, Custo A, Grouiller F, Schneider M, Debbané M, Eliez S, Michel CM (2014) Deviant dynamics of EEG resting state pattern in 22q11.2 deletion syndrome adolescents: A vulnerability marker of schizophrenia? Schizophr Res 157:175–181.

Tzourio-Mazoyer N, Landeau B, Papathanassiou D, Crivello F, Etard O, Delcroix N, Mazoyer B, Joliot M (2002) Automated Anatomical Labeling of Activations in SPM Using a Macroscopic Anatomical Parcellation of the MNI MRI Single-Subject Brain. Neuroimage 15:273–289.

Villalón-Reina JE et al. (2019) Altered white matter microstructure in 22q11 . 2 deletion syndrome : a multisite diffusion tensor imaging study. Mol Psychiatry.

Vrba J (2002) Magnetoencephalography: The art of finding a needle in a haystack. Phys C Supercond its Appl 368:1–9.

Warland A, Kendall KM, Rees E, Kirov G, Caseras X (2019) Schizophrenia-associated genomic copy number variants and subcortical brain volumes in the UK Biobank. Mol Psychiatry:1.

Zinkstok J, Amelsvoort T van (2005) Neuropsychological Profile and Neuroimaging in Patients with 22Q11.2 Deletion Syndrome: A Review. Child Neuropsychol 11:21–37.